

Capacity Analysis for Closed and Open Access Femto Cell Networks

Pawel A. Dmochowski* Peter J. Smith†, Mansoor Shafi‡

* School of Engineering and Computer Science, Victoria University of Wellington, Wellington, New Zealand

† Department of Electrical and Computer Engineering, University of Canterbury, Christchurch, New Zealand

‡ Telecom New Zealand, Wellington, New Zealand

Email: pawel.dmochowski@vuw.ac.nz, p.smith@elec.canterbury.ac.nz, mansoor.shafi@telecom.co.nz

Abstract—We investigate the performance of femto cell networks in both closed and open access regimes. Specifically, we analyse the typical user capacity as well as the sum capacity of all users in a macro cell with a Poisson field of femto base stations. The closed access results demonstrate that while the system sum capacity initially increases with the density of femto cells, this gain comes with a significant performance penalty suffered by an individual macro user. In open access mode, we show via analytical derivations that macro users only benefit from access to the available femto base stations for impractically high densities. Furthermore, we derive limiting sum capacity results showing that while the mean sum capacity initially increases linearly with femto density, sum capacity will eventually decay to zero in the limiting case as the femto density approaches infinity.

I. INTRODUCTION

Wireless data traffic is doubling every year resulting in a 1000 times growth over the past 10 years. However, the bulk of this data traffic is indoors. This means that hand off requirements for the 'stationary' indoor traffic are not as critical as for the 'truly' mobile traffic. There are a number of ways to off load traffic from the macro network (that supports hand off and mobility) to other platforms; these include WiFi, femto cells (known also as Home e-Node B's, HeNBs) etc. The focus of this paper is on the latter. The HeNBs are low power (typically +10 dBm) base stations [1], back hauled via the fixed broadband access network to the mobile core network via an optional HeNB gateway. Mobility to/from E-UTRAN to the HeNB is supported but intra HeNB mobility is not supported [2]. Due to the short transmission/receive distance the femto cell user can enjoy a higher signal-to-interference-and-noise ratio (SINR), and therefore higher data rates, as compared to the macro users. Increasing the density of femto cells, therefore, can result in achieving very high throughputs - potentially hundreds of Mbits/s/Hz over a given area [3], [4]. This is, of course, true only if femto-femto interference and femto-macro interference does not pose any limitation. Past studies have shown that femto-femto interference is limited as the femto cells are in doors and the wall loss limits the interference. It has also been suggested that there is only a marginal impact on the macro capacity due to the femto interference [5]. On the other hand, some studies have also shown that the macro capacity could suffer a substantial loss due to the femto interference [6]. Some studies have considered the interference but have not fully considered all

aspects of the fading channel, i.e. either ignored the shadow fading [7], [8] or ignored the fast fading [5]. The investigation of these issues is the main theme of this paper. We have considered all aspects of fading (distance dependence, fast fading, shadow fading) and developed expressions for the SINR of femto and macro cells for both open and closed access. The SINR is then used to estimate capacity and a capacity loss due to interference.

The contributions of the paper are as follows:

- We derive new limiting results for the sum capacity of high density femto cell systems. These results reveal that while for small femto densities the system performance increases linearly with femto density, the limiting total capacity for high femto densities tends to zero as a result of interference.
- We show that while the system capacity increases for moderate increases in femto density, the capacity of a single macro user degrades significantly as a result of the additional interference. The corresponding drop for a typical femto user is less pronounced due to the propagation characteristics. Furthermore, we show that this performance drop is very sensitive to the pathloss exponent and shadowing variance.
- Through analytical derivations we show that macro user will only benefit from available femto base stations in open access mode for very large femto densities.

The paper is laid out as below. In Section II we describe the system model for open and closed access schemes. Section III presents the analytical results for sum capacity in the limit of high femto density. Section IV gives the simulation results and discussion, including the femto density requirements for improved macro user performance. Finally, in Section V the conclusions of the paper are given.

II. SYSTEM MODEL

The system model is depicted in Fig. 1. In our study, we do not consider the problem of user scheduling and focus on the system performance *per system resource*. In the context of 4G systems this could be an LTE resource block. Thus, the system parameters described henceforth are defined *per system resource*. The macrocell base station is located at the origin of a circular coverage area with radius R . Within this area we consider N_{mu} macro users drawn from a 2-D Poisson Point

Process with intensity $\lambda_m = \Phi_m \pi R^2$, where Φ_m denotes the mean macro user density. Similarly, the femtocell base stations are drawn from a 2-D Poisson Point Process with intensity $\lambda_f = \Phi_f \pi R^2$ where Φ_f denotes the mean femto cell density. To account for out-of-cell interference, we also consider femto base stations located in an annular region of radius $R < r < R_o$, and assume the same density Φ_f . Denoting by N' and N'_o the total number of physical femto cells inside and outside the coverage area, respectively, we model the femto occupancy by an activity factor p_{act} . Hence, the number of femto cells operating inside the coverage area is denoted N and satisfies $\mathbb{E}(N) = p_{\text{act}} N'$. Similarly, N_o operate in the annulus outside where $\mathbb{E}(N_o) = p_{\text{act}} N'_o$ and both N and N_o are binomial for given values of N' and N'_o . For each active femto cell the corresponding user is randomly located within a femto cell coverage area of radius r_f . We denote the total number of femto base stations by $N_{\text{tot}} = N + N_o$.

-  N FBSs inside coverage area
-  N_o FBSs outside coverage area
-  N_{mu} MUs inside cov. area
-  N_{fu} FUs inside cov. area

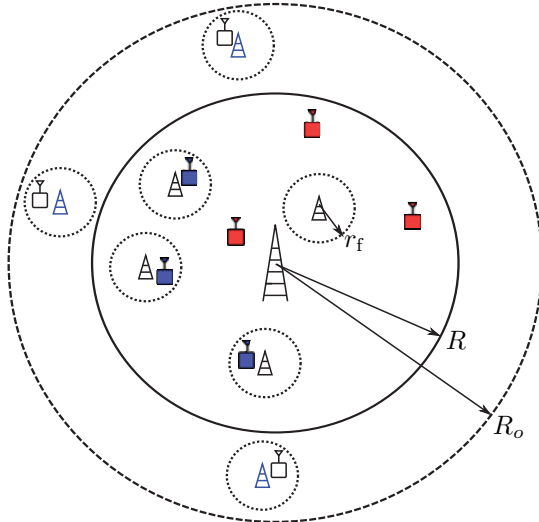


Fig. 1. System Diagram

All channels follow the classic pathloss and Rayleigh fading model, where, denoting the macro and femto quantities by subscripts m and f , respectively, the instantaneous received power is given by

$$P_r = P_t d^{-\gamma} L W |h|^2. \quad (1)$$

In (1), $P_t \in \{P_{t,m}, P_{t,f}\}$ denotes the transmit power, d is the distance separating the transmitter and receiver, $\gamma \in \{\gamma_m, \gamma_f\}$ is the pathloss exponent, L is the lognormal shadowing with variance σ_{sf}^2 (assumed equal for macro and femto users), W is the wall loss and h is a zero mean circularly symmetric complex Gaussian random variable with unit variance.

We assume that the femto users are located indoors with a probability p_{ind} , while the macro user is assumed to be located outdoors. The transmit powers of macro and femto BSs are

set such that the average signal-to-noise ratio (SNR) satisfies the probability

$$\Pr \left\{ \overline{\text{SNR}} > \gamma_T \right\} = \alpha, \quad (2)$$

where γ_T is a predefined SNR threshold and α is the reliability. The long term SNR, $\overline{\text{SNR}} \in \{\overline{\text{SNR}}_m, \overline{\text{SNR}}_f\}$ is given by

$$\overline{\text{SNR}} = \frac{P_t d^{-\gamma} L W}{\sigma^2}, \quad (3)$$

with σ^2 denoting the AWGN variance at the receiver. Furthermore, we impose a limit on macro BS transmit power effectively limiting the average received SNR to some $\overline{\text{SNR}}_{m,\text{max}}$.

The instantaneous signal-to-interference-and-noise ratio (SINR) for the macro user assigned to the macro BS is given by

$$\text{SINR}_m = \frac{P_{r,m}}{\sigma^2 + \sum_{j=1}^{N_{\text{tot}}} I_{f_j,m}}, \quad (4)$$

where $P_{r,m}$ is given by (1), with $d = d_m$ denoting the distance from macro BS to macro user. The interference term $I_{f_j,m}$ in (4) denotes the interference from j th femto base station to the macro user, and is given by

$$I_{f_j,m} = P_{t,f} d_{f_j,m}^{-\gamma_m} L_{f_j,m} W_{f_m} |h_{f_j,m}|^2, \quad (5)$$

where the wall loss $W_{f_m} = W$ is constant for all j as all femto base stations are assumed to be indoors while the macro users are assumed to be outdoors.

Similarly, the SINR for a femto user i is given by

$$\text{SINR}_{f_i} = \frac{P_{r,f_i}}{\sigma^2 + \sum_{j=1, j \neq i}^{N_{\text{tot}}} I_{f_j,f_i} + I_{m_i}}, \quad (6)$$

where the desired received signal power at femto user i , P_{r,f_i} , is given by (1), with $d = d_{f_i}$ denoting the distance from femto base station to the desired femto user, and $W = W_{f_i}$ is

$$W_{f_i} = \begin{cases} 0 & \text{if FU } i \text{ indoor} \\ W & \text{if FU } i \text{ outdoor.} \end{cases} \quad (7)$$

Similarly, the femto BS to femto user interference, I_{f_j,f_i} , in (6) is given by

$$I_{f_j,f_i} = P_{t,f} d_{f_j,f_i}^{-\gamma_m} L_{f_j,f_i} W_{f_i} |h_{f_j,f_i}|^2, \quad (8)$$

where d_{f_j,f_i} denotes the distance from an interfering femto BS j to femto user i , and the associated wall loss $W = W_{f_i}$ is

$$W_{f_j,f_i} = \begin{cases} 2W & \text{if FU } i \text{ indoor} \\ W & \text{if FU } i \text{ outdoor.} \end{cases} \quad (9)$$

Finally, the second interference term in the denominator of (6), I_{m_i} , is

$$I_{m_i} = P_{t,m} d_{m_i}^{-\gamma_m} L_{m_i} W_{m_i} |h_{m_i}|^2, \quad (10)$$

where d_{mf_i} denotes the distance from macro BS to femto user i and the wall loss $W = W_{mf_i}$ given by

$$W_{mf_i} = \begin{cases} W & \text{if FU } i \text{ indoor} \\ 0 & \text{if FU } i \text{ outdoor.} \end{cases} \quad (11)$$

Given the SINR definitions in (4) and (6), we have the macro user capacity per unit bandwidth given by

$$C_m = \log_2(1 + \text{SINR}_m) \quad (12)$$

and the sum capacity for femto users within radius R is

$$C_{f,\text{tot}} = \sum_{i:d_{mf_i} < R} \log_2(1 + \text{SINR}_{f_i}). \quad (13)$$

A. Closed Access

Under the closed access system, each femto cell is associated with a predefined set of femto users that have been granted access by the femto BS owner. Consequently, in our model, where performance per system resource is considered, we assume the femto base station is transmitting to a single user within its coverage radius r_f . Similarly, a single macro user within the coverage area of radius R is served by the macro base station and does not have access to any of the N' physical femto base stations regardless of their proximity, activity or signal strength.

B. Open Access

In contrast, in an open access system, we assume that any of the N_{mu} macro users and N femto users are permitted to be served by the macro BS or an available femto BS¹. Consequently, we assume a random arrival order for all users and assign each to either the macro BS or any of the N' femto BSs associated with the strongest average signal level. This will include the $N' - N$ available femto BSs with no local femto users². Once a base station is assigned to a particular user, it is considered to be unavailable.

III. LIMITING CAPACITY RESULTS

In this section, we consider the effect of increasing the femto density, Φ_f , on the macro capacity, C_m , and the sum capacity for the femto users, $C_{f,\text{tot}}$. We consider the fixed coverage area described in Section II and the closed access system. In particular, we investigate the behaviour of C_m and $C_{f,\text{tot}}$ as $\Phi_f \rightarrow \infty$.

Results for C_m are obvious. From (12) and (4) it follows that $\text{SINR}_m \rightarrow 0$ as $\Phi_f \rightarrow \infty$ and so $C_m \rightarrow 0$. Clearly, as the femto density is increased, the number of interferers grows and the capacity of the single macro user link decays to zero.

Results for $C_{f,\text{tot}}$ are less obvious as there are competing factors at play. As Φ_f increases, the number of terms in (13) increases which helps to boost capacity. However, each femto user also suffers more interference as in (6). Hence, although

¹In the context of an open access system, the activity factor p_{act} represents the probability that a local femto user is seeking access to its femto BS.

²While in reality the femto users could connect to femto BSs outside the coverage radius R , the potential performance difference represents an edge effect which we neglect in the interest of model simplicity.

there are more terms in (13), each term tends to be smaller. To make progress in this scenario, we assume that $\gamma_f = 4$, the wall loss is fixed for all femto-femto links, the shadow fading standard deviation is constant for all femto-femto links and the transmit power is fixed for all femto BSs. In this simplified scenario, there are N femtocell base stations inside the coverage area so that, using (13),

$$\mathbb{E}[C_{f,\text{tot}}] = \mathbb{E}(N)\mathbb{E}[\log_2(1 + \text{SINR}_{f_i})]. \quad (14)$$

Since the femtocell base stations form a 2-D Poisson process in the coverage area, it follows that $E(N) = \Phi_f \pi R^2$. Next, we rewrite (8) as $I_{f_j f_i} = \Gamma_j |h_{ji}|^2$. With this notation, SINR_{f_i} is written as

$$\text{SINR}_{f_i} = \frac{P_{r,f_i}}{\sigma^2 + \sum_{j=0}^{N_{\text{tot}}} \Gamma_j |h_{ji}|^2 + I_{m_i}}. \quad (15)$$

Now, using Jensen's inequality

$$\begin{aligned} \mathbb{E}[C_{f,\text{tot}}] &\leq \Phi_f \pi R^2 \log_2(1 + \mathbb{E}[\text{SINR}_{f_i}]) \\ &< \Phi_f \pi R^2 \log_2 \left(1 + \mathbb{E}(P_{r,f_i}) \mathbb{E} \left[\left(\sum_{j=0}^{N_{\text{tot}}} \Gamma_j |h_{ji}|^2 \right)^{-1} \right] \right). \end{aligned} \quad (16)$$

The argument of the second expectation in (16) can be written as

$$\left(\sum_{j=0}^{N_{\text{tot}}} \Gamma_j \right)^{-1} \left(\sum_{j=0}^{N_{\text{tot}}} \frac{\Gamma_j}{\sum_{k=0}^{N_{\text{tot}}} \Gamma_k} |h_{ji}|^2 \right)^{-1}. \quad (17)$$

By a version of the law of large numbers [9], the second term in (17) is a weighted average of iid exponentials of unit mean and hence converges to 1 as $R_o \rightarrow \infty$ and hence $N_{\text{tot}} \rightarrow \infty$. As $R_o \rightarrow \infty$ and an infinite plane of interferers is considered, it is known that the limiting distribution of $Y = \sum_{j=0}^{N_{\text{tot}}} \Gamma_j$ is Levy [10] with probability density function [11]

$$f_Y(y) = \sqrt{\frac{\delta}{2\pi}} \frac{e^{-\delta/2y}}{y^{3/2}}, \quad y > 0 \quad (18)$$

where $\delta = \frac{1}{2} P_{t,f} W_{f_j f_i} \pi^2 \Phi_f^2 \Gamma(1/2) \exp(\tilde{\sigma}^2/4)$ and $\tilde{\sigma} = \log_e(10)\sigma/10$. It is shown in [11] that Y is an example of an inverse gamma variable and some straightforward transformation theory for random variables shows that

$$Y = \Phi_f^2 X^{-1} \quad (19)$$

with X a gamma variable with shape parameter 1/2 and scale parameter $\frac{1}{4} P_{t,f} W_{f_j f_i} \pi^2 \exp(\tilde{\sigma}^2/4)$ which is independent of Φ_f . Substituting (6) and (17) into (16) gives

$$\begin{aligned} &\lim_{R_o \rightarrow \infty} \{\mathbb{E}[C_{f,\text{tot}}]\} \\ &< \lim_{R_o \rightarrow \infty} \left\{ \Phi_f \pi R^2 \log_2 \left(1 + \mathbb{E}(P_{r,f_i}) \mathbb{E}(X) \Phi_f^{-2} \right) \right\} \\ &\leq \lim_{R_o \rightarrow \infty} \left\{ \pi R^2 \mathbb{E}(P_{r,f_i}) \mathbb{E}(X) \Phi_f^{-1} \right\}. \end{aligned} \quad (20)$$

TABLE I
SYSTEM PARAMETERS

Parameter	Value
FBS coverage radius, r_f	20 m
MBS coverage radius, R	1 km
radius encompassing out of cell interference, R_o	2 km
femto activity factor, p_{act}	0.25
indoor user probability, p_{ind}	0.5
macro pathloss exponent, γ_m	3.4
femto pathloss exponent, γ_f	3
shadowing variance, σ_{sf}	8,10 dB
target SNR, γ_T	10 dB
SNR reliability, α	95%
max mean received MU SNR, $\text{SNR}_{m,max}$	20 dB
wall loss, W	10 dB

Since, the right hand side of (20) decreases with Φ_f it follows that $\lim_{\Phi_f \rightarrow 0} \lim_{R_o \rightarrow \infty} \{\mathbb{E}[C_{f,tot}]\} = 0$.

Hence, when an infinite field of femto base stations is considered ($R_o \rightarrow \infty$) in the limit as you increase Φ_f , the sum capacity of the femto users decays to zero in any given coverage area.

Consider the opposite case where $\Phi_f \rightarrow 0$. Here, as $R_o \rightarrow \infty$ we have from (15), (17) and (19)

$$\text{SINR}_{f_i} \rightarrow \frac{P_{r,f_i}}{\sigma^2 + \Phi_f^2/X + I_{m_i}} \quad (21)$$

and as $\Phi_f \rightarrow 0$ it follows that $\text{SINR}_{f_i} \rightarrow P_{r,f_i}(\sigma^2 + I_{m_i})^{-1}$. Hence, for small Φ_f , the log term in (14) is approximately constant while $\mathbb{E}(N) = \Phi_f \pi R^2$ grows linearly with Φ_f .

In summary, $\mathbb{E}(C_{f,tot})$ grows linearly with Φ_f for small Φ_f and decays to zero as $\Phi_f \rightarrow \infty$.

IV. SIMULATION RESULTS

In this section, we present simulation results for open and closed access schemes as described in Sections II-A and II-B. Unless otherwise indicated in the figures, the values of system parameters used are listed in Table I.

Figure 2 plots the closed access capacity cdf for the MU and a typical (randomly selected) FU, calculated using (12) and a single summation term in (13), respectively, for varying FU density Φ_f . A reference plot of MU capacity with no femto cells ($\Phi_f = 0$) is also shown. The figure shows the significant degradation in MU capacity resulting from the femto interference. We note that while the interference causes the capacity of a single FU to decline, this loss is significantly less pronounced. This difference can be attributed to the wall loss reducing the interference term in (6).

More insight into the capacity loss of the MU can be gained from Fig. 3, which shows the percentage drop in the mean MU capacity as a function of Φ_f for different propagation parameters. We observe the extreme sensitivity of the loss to the pathloss exponent, where for $\gamma_m = 3$ the MU suffers a significantly greater loss compared to $\gamma_m = 4$. This makes the system design a very delicate task since the performance varies rapidly with the propagation environment.

While the individual user capacity drops with a higher density of femtos, Fig. 3 shows that the overall system capacity,

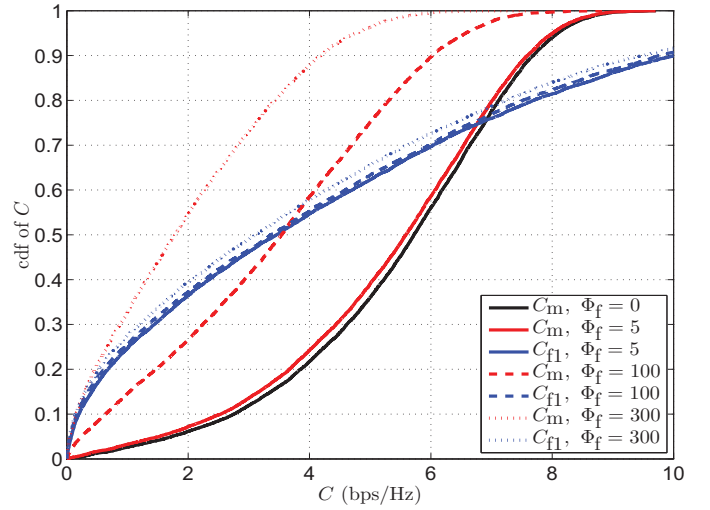


Fig. 2. Typical user (femto and macro) capacity cdf (closed access, $\gamma_m = 3$, $\sigma_{sf} = 8$ dB).

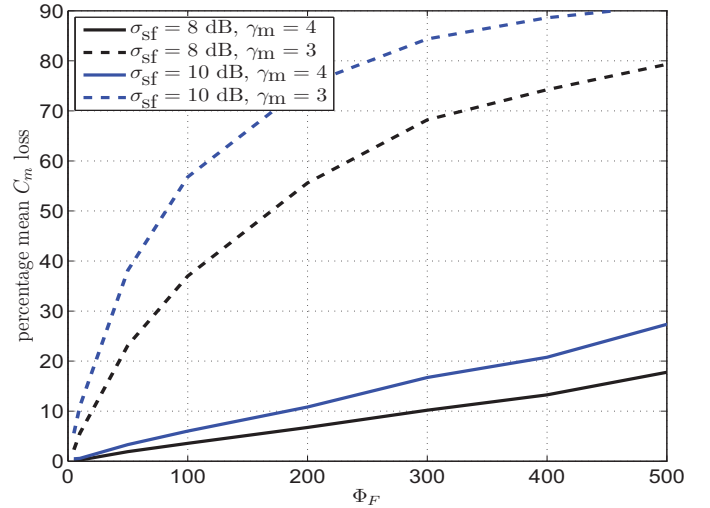


Fig. 3. Percentage loss in mean MU capacity due to femto interference (closed access).

$C_{tot} = C_{f,tot} + C_m$, continues to increase for the range of Φ_f plotted for both closed and open access regimes. The plot reveals an approximately linear increase in sum capacity for the range of femto densities considered.

Figure 5 shows the open access capacity cdf of a typical MU, along with a reference curve for the closed access MU capacity. The results include the performance of MU attached to a macro BS as well as opportunistic MUs accessing open femto BSs. We note that while allowing MUs access to open femto BSs increases the number of MUs that can access the system, their performance is significantly degraded.

Figures 6 and 7 show the cdf of SNR and distance to the BS, respectively, for the four scenarios in an open access system with femto density $\Phi_f = 100$. We note that due to the distance

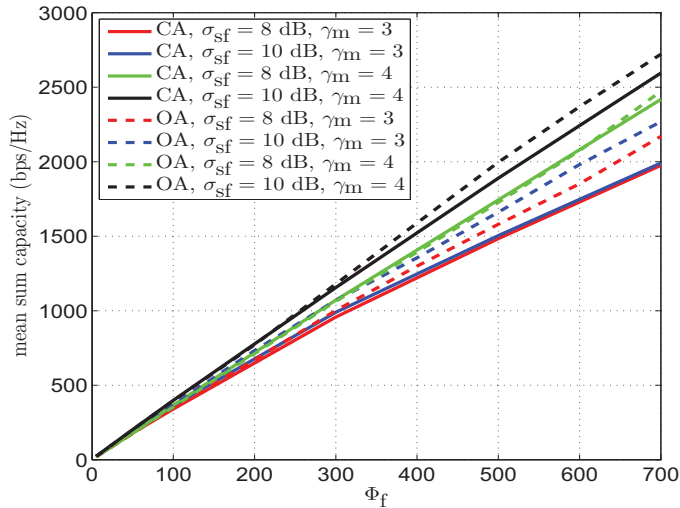


Fig. 4. Mean system capacity wrt $\Phi_f = 5$ (closed and open access, $\Phi_m = 1$)

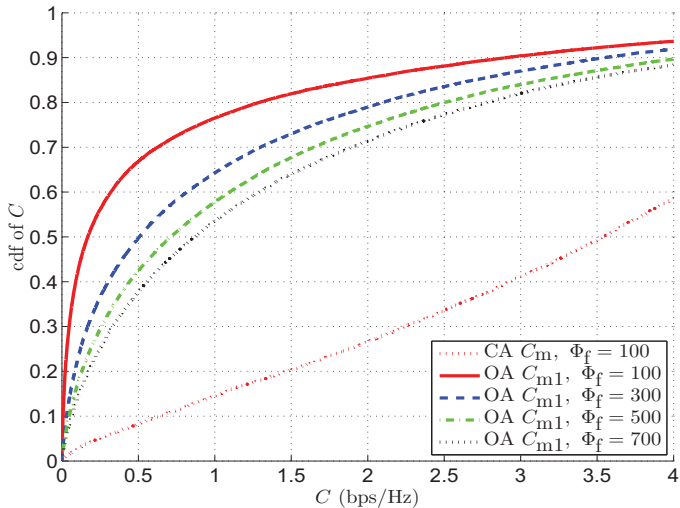


Fig. 5. Typical MU capacity (open access, $\Phi_m = 1$, $\gamma_m = 3$, $\sigma_{sf} = 8$ dB).

to the FBS and the low transmit power of the femtos, the SNR of the MU served by FBS is significantly lower than that of the other three scenarios.

The statistics of the minimum distance d_{\min} of the MU to a FBS for different femto densities can be derived as follows. For femto BS following a Poisson Point Process with density Φ_f , we have the probability $\mathbb{P}(d_{\min} > x) = e^{-\Phi_f \pi x^2}$. Thus, we have

$$\mathbb{P}(d_{\min} < x) = 1 - e^{-\Phi_f \pi x^2} \quad (22)$$

where the corresponding pdf is $f(x) = \Phi_f \pi 2x e^{-\Phi_f \pi x^2}$. Taking the expectation of d_{\min} gives, after trivial manipulation,

$$\mathbb{E}(d_{\min}) = \frac{1}{2\sqrt{\Phi_f}}. \quad (23)$$

Thus, assuming a femto coverage radius $r = 20$ m, we require a femto density of $\Phi_f = 625$ in order to offer the MU a similar link distance. We note, however, that (23) yields an optimistic result, since, unlike in the model considered, it assumes all femto BSs to be available to the MU. Figure 8 shows the cdf

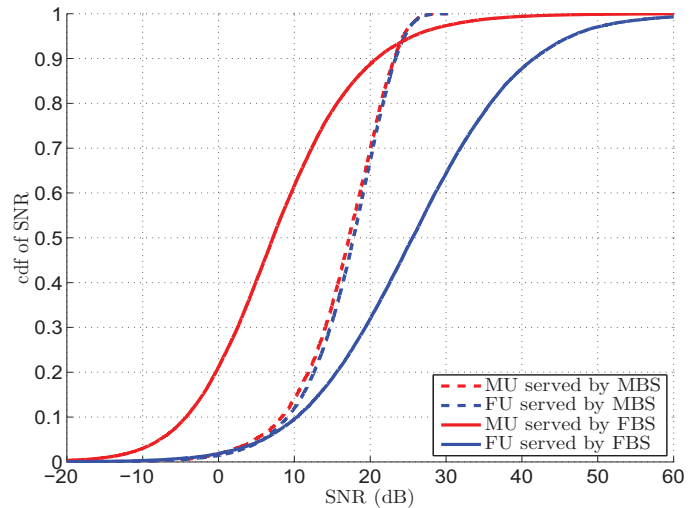


Fig. 6. SNR cdfs (open access, $\Phi_f = 100$, $\Phi_m = 1$, $\gamma_m = 3$, $\sigma_{sf} = 8$ dB).

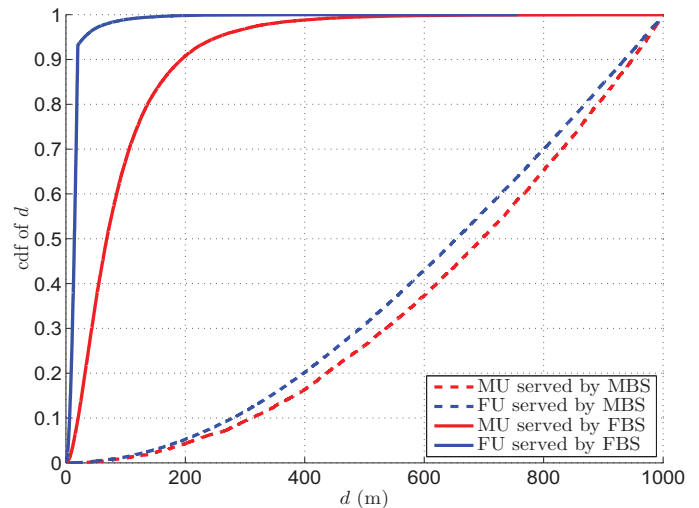


Fig. 7. Distance cdfs (open access, $\Phi_f = 100$, $\Phi_m = 1$, $\gamma_m = 3$, $\sigma_{sf} = 8$ dB).

of the average MU-FBS distance in an open access system for varying Φ_f . For femto density $\Phi_f = 700$ we observe a mean distance of approximately 25 meters. As discussed, the discrepancy between the result of the simulation and the result predicted by (23) ($\mathbb{E}(d_{\min}) = 18.9$ m for $\Phi_f = 700$) is attributed to the fact that the simulations represent the minimum distance to *available* femto BSs, ie those not already assigned to previous users. Despite this difference, the results indicate that while the open access model allows additional

MUs to obtain service, impractically high femto densities are required in order to provide a quality of service comparable to that of a MU-MBS link.

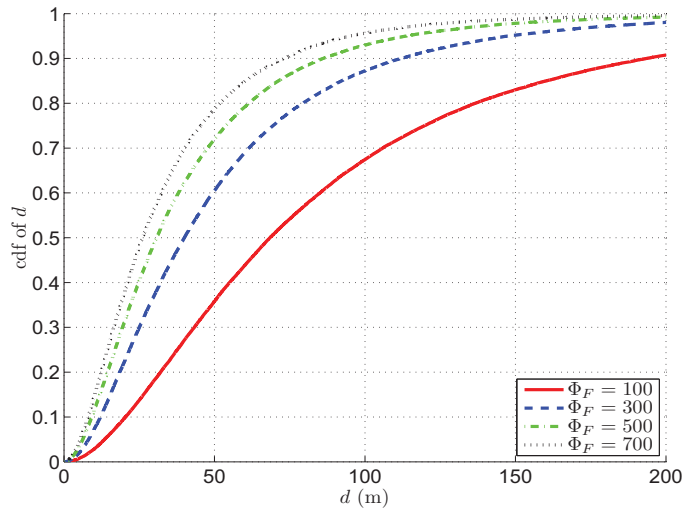


Fig. 8. Distance cdf for MU-FBS (open access, $\Phi_m = 1$, $\gamma_m = 3$, $\sigma_{sf} = 8$ dB).

V. CONCLUSIONS

We have presented a study of the femto cell system performance for closed and open access modes. We have shown that the increase in overall system throughput resulting from additional femto BSs comes at a significant performance penalty to a typical macro user. We have shown via analysis and simulation that while an open access system enables more macro users to obtain service, very large femto densities are required to provide performance comparable to that offered by a macro BS link. Furthermore, we have shown that while the initial increase in femto density results in improved system capacity, the sum capacity tends to zero in the limit of increasing femto density.

REFERENCES

- [1] 3GPP TSG-RAN WG4 Meeting #43bis, "Home Node B output power," June 2007.
- [2] 3GPP TR 23.830, "Architecture aspects of home NodeB and home eNodeB (release 9)," Tech. Rep., March 2009.
- [3] V. Chandrasekhar, J. Andrews, and A. Gatherer, "Femtocell networks: a survey," *IEEE Communications Magazine*, vol. 46, no. 9, pp. 59–67, 2008.
- [4] J. G. Andrews, H. Claussen, M. Dohler, S. Rangan, and M. C. Reed, "Femtocells: Past, present, and future," *To appear, IEEE Journal on Sel. Areas in Comm.*, Mar. 2012.
- [5] H. Claussen, "Performance of macro-and co-channel femtocells in a hierarchical cell structure," in *IEEE 18th International Symposium on Personal, Indoor and Mobile Radio Communications*, 2007, pp. 1–5.
- [6] 3GPP TSG-RAN WG4 Meeting #43bis, "Initial home NodeB coexistence simulation results," June 2007.
- [7] H. Jo, P. Xia, and J. Andrews, "Downlink femtocell networks: Open or closed?" in *Proc. IEEE International Conference on Communications (ICC)*, Kyoto, June 2011, pp. 1–5.
- [8] H. S. Dhillon, R. K. Ganti, F. Baccelli, and J. G. Andrews, "Modeling and analysis of K-tier downlink heterogeneous cellular networks," *To appear, IEEE Journal on Sel. Areas in Comm.*, Mar. 2012.
- [9] I. Ahmad, "An almost sure convergence theorem for weighted sum of random elements in separable banach spaces with random weights," *Sankhyā: The Indian Journal of Statistics, Series A (1961-2002)*, vol. 44, no. 2, pp. 262–268, Jun. 1982.
- [10] X. Hong, C. Wang, and J. Thompson, "Interference modeling of cognitive radio networks," in *Proc. IEEE Vehicular Technology Conference (VTC Spring)*, Singapore, May 2008, pp. 1851–1855.
- [11] P. Dmochowski, P. Smith, M. Shafi, J. Andrews, and R. Mehta, "Interference models for heterogenous sources," in *Proc. International Conference on Communications (ICC)*, Ottawa, June 2012.